ACS Catalysis

Letter

pubs.acs.org/acscatalysis

Visible Light-Driven Water Splitting in Photoelectrochemical Cells with Supramolecular Catalysts on Photoanodes

Xin Ding,[†] Yan Gao,*[,†] Linlin Zhang,[†] Ze Yu,[†] Jianhui Liu,[†] and Licheng Sun*[,†,‡]

[†]State Key Laboratory of Fine Chemicals, Institute of Artificial Photosynthesis, DUT-KTH Joint Education and Research Center on Molecular Devices, Dalian University of Technology (DUT), Dalian 116024, China

[‡]Department of Chemistry, School of Chemical Science and Engineering, KTH Royal Institute of Technology, 100 44 Stockholm, Sweden

Supporting Information

ABSTRACT: By using a supramolecular self-assembly method, a functional water splitting device based on a photoactive anode TiO_2(**1**+**2**) has been successfully assembled with a molecular photosensitizer **1** and a molecular catalyst **2** connected by coordination of **1** and **2** with Zr^{4+} ions on the surface of nanostructured TiO_2. On the basis of this photoanode in a three-electrode photoelectrochemical cell, a maximal incident photon to current conversion efficiency of 4.1% at ~450 nm and a photocurrent density of ~0.48 mA cm^{-2} were successfully obtained

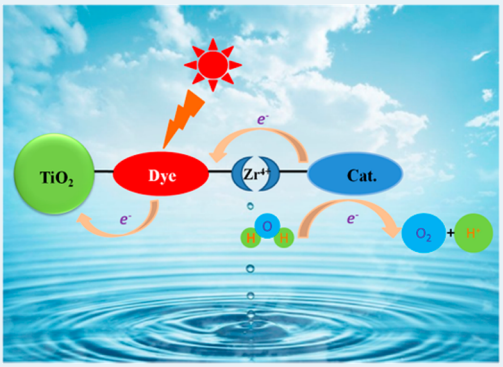

KEYWORDS: *water splitting, molecular catalyst, visible light, photoanode, water oxidation*

The conversion of solar energy into chemical energy, in the forms of hydrogen, for example, via visible light-driven water splitting, is regarded as an ideal solution to meet future energy demands.[1] Photoelectrochemical cells (PECs) as a feasible way to realize water splitting have been designed and assembled progressively in recent years.[2−19] Most PECs have been assembled using inorganic materials,[2−11] and only a few PECs composed of molecular components have been developed.[12−19] However, PECs with molecular devices such as photoanodes usually display low conversion efficiencies for light-driven water splitting. One major reason is the inefficient water oxidation catalysts used in the molecular devices.[12−18] Assembly methods of photoanodes may also play an important role in determining the light to hydrogen conversion efficiencies of PECs.[2,13,14,19]

In general, there are two methods that can be employed to design a photoanode based on a nanostructured n-type semiconductor, such as TiO_2, as shown in Chart 1. The first method (method I) is to incorporate both a catalyst and a photosensitizer (PS) on the TiO_2 surface in one dyeing bath, forming a one-layer anode.[12,19] Another method (method II) is to covalently link a catalyst to a PS. Anchoring groups on the other side of the PS facilitate the assembly of the formed supramolecular system on the surface of TiO_2. In method I, the catalyst and the PS are randomly distributed on the surface of TiO_2. In method II, however, the PS is assembled closely on the surface of TiO_2, and the catalyst is removed (forced) to separate from the surface of TiO_2 due to the nature of chemical bonding between the two units. One advantage of method II over method I is that the charge recombination between the injected electrons in the conduction band of TiO_2 and the oxidized forms of the catalyst might become retarded because of the separation of the catalyst from the surface of TiO_2 by the PS.

Chart 1. Two Methods for Assembling Photoanodes of PECs

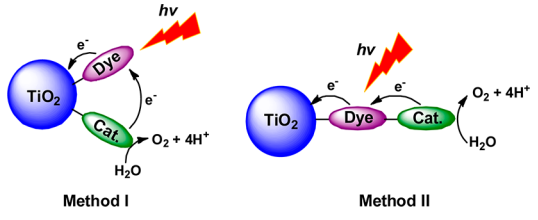

In recent years, a series of highly efficient water oxidation ruthenium-based catalysts have been developed in our group.[20−23] On the basis of one of the efficient catalysts and a molecular photosensitizer, a functional photoelectrochemical device has been successfully assembled according to method I.[19] The PEC using this molecular device as a photoanode displayed an unprecedented high photocurrent density on light-driven water splitting.[19] However, with assembly method I, the

Received: April 18, 2014
Revised: June 13, 2014
Published: June 13, 2014

   dx.doi.org/10.1021/cs500518k | ACS Catal. 2014, 4, 2347−2350

catalyst in this molecular device is directly assembled on the surface of TiO_2, and the catalytic center is close to TiO_2. Charge recombinations between the conduction band electrons in TiO_2 and the oxidized forms of the catalyst seem to be difficult to avoid.

Here, we introduce another functional photoanode assembled through the supramolecular self-assembly method using a similar molecular catalyst and a PS as we reported previously.[13,19] Inspired by a previous work reported by Meyer et al.,[17] we used a Zr^{4+} ion as a linkage to connect a molecular catalyst **2** and a molecular PS **1** in the photoanode, as shown in Scheme 1. The photoelectrochemical properties of this new type of photocathode were systematically studied in this work.

Scheme 1. Illustration of the PEC with a Photoanode Assembled from PS $[Ru(4,4\text{-}(PO_3H_2)_2bpy)_3]Cl_2$ (1), Zr^{4+} Ion and a Molecular Ru Catalyst (2) on Nanostructured TiO_2 [TiO_2(1+2)], and a Passive Pt Cathode, for Visible Light-Driven Water Splitting in an Aqueous Solution

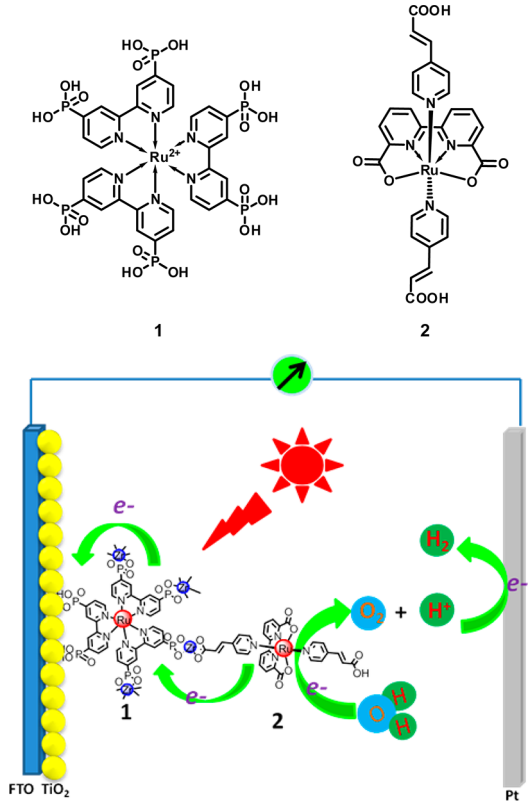

Following the approach developed by Haga et al.,[26] the photoanode was prepared according to a previously reported method.[17] With a 0.1 M $HClO_4$ aqueous solution as a solvent, the TiO_2-sintered FTO electrode was immersed in the solution containing 1 mM PS **1** for 12 h to obtain working electrode (WE) TiO_2(**1**). Then it was immersed stepwise in the solution containing 1 mM $ZrOCl_2$ and the solution containing 1 mM catalyst **2** for 12 h each to produce the desired WE TiO_2(**1**+**2**) (see Scheme 1). As a reference, a WE TiO_2(**1**+**2a**) was also assembled in a analogous method, in which Zr^{4+} ion treatment is absent. For the purpose of comparison, the TiO_2-sintered FTO electrode adsorbed with only catalyst **2** [TiO_2(**2**)] was also prepared as a reference. Cyclic voltammetric (CV) measurements of WEs TiO_2(**1**+**2**), TiO_2(**1**+**2a**) (as shown in Figure 1), TiO_2(**1**), and TiO_2(**2**) (as shown in Figure S1 of the

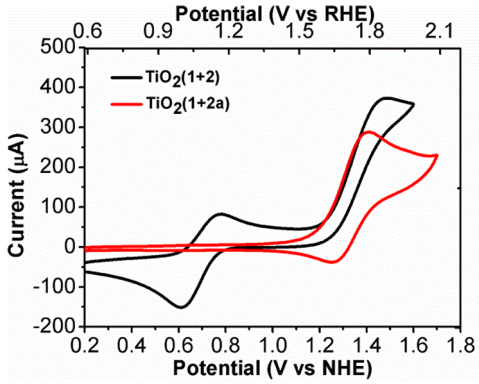

Figure 1. Cyclic voltammograms of working electrode TiO_2(**1**+**2**) treated with Zr^{4+} (black line) and TiO_2(**1**+**2a**) treated without Zr^{4+} (red line) in a 0.1 M Na_2SO_4 (pH 6.4) solution using Ag/AgCl as the reference electrode and Pt as the counter electrode, with a scan rate of 100 mV/s ($E_{NHE} = E_{Ag/AgCl} + 0.20$ V, and $E_{RHE} = E_{Ag/AgCl} + 0.20$ V + 0.0591 × pH).

Supporting Information) were implemented in a 0.1 M Na_2SO_4 solution at pH 6.4. A reversible peak observed at an $E_{1/2}$ of 0.68 V [vs the normal hydrogen electrode (NHE)] for WE TiO_2(**1**+**2**) (black line in Figure 1) is assigned to the oxidation potential of Ru^{II}/Ru^{III} for catalyst **2**. An irreversible oxidation peak observed at an E_{pa} of 1.40 V (vs the NHE) is assigned to the redox couple of Ru^{II}/Ru^{III} for PS **1**. The oxidation potential of Ru^{II}/Ru^{III} is higher than the onset potential for catalytic water oxidation at 1.20 V (vs the NHE), indicating that this electrode can be thermodynamically used for visible light-driven water splitting. The surface loadings of PS **1** and catalyst **2** on WE TiO_2(**1**+**2**) were estimated with the peaks area of Ru^{II}/Ru^{III} of 0.68 and 1.4 V to be 2.01×10^{-9} and 1.84×10^{-9} mol/cm^2, respectively, in a molar ratio of ~1:1.[24,25]

In comparison, CV measurement of WE TiO_2(**1**+**2a**) without Zr^{4+} ion has also been performed (Figure 1, red line). The potential at ~1.35 V (vs the NHE) is found to be a strong peak of the Ru^{II}/Ru^{III} redox process of PS **1**; however, the potential at an $E_{1/2}$ of 0.68 V (vs the NHE) is found to be a very weak peak of the Ru^{II}/Ru^{III} redox couple of catalyst **2**. Via comparison of the Ru^{II}/Ru^{III} redox peaks at either 1.4 or 0.68 V, the amounts of PS **1** on the two WEs are found to be analogous, whereas the amount of catalyst **2** on WE TiO_2(**1**+**2a**) is found to be much smaller than that on WE TiO_2(**1**+**2**). These results imply a limited amount of catalyst adsorbed on the WE in the absence of Zr^{4+} ion and indicate that Zr^{4+} ion is indispensable for connecting PS **1** and catalyst **2** in this type of molecular device. The results also reflect the fact that Zr^{4+} ion really exists as a linker to connect PS **1** and catalyst **2** in WE TiO_2(**1**+**2**).[24,25]

A three-electrode PEC consisted of WE TiO_2(**1**+**2**) as a photoanode, Ag/AgCl as a reference electrode, and platinum (Pt) wire as a cathode. The PEC was illuminated with visible light (>400 nm, 300 mW/cm^2) in a 0.1 M Na_2SO_4 solution, applying different external biases (vs the NHE) as shown in Figure 2. When a 0 V external bias is applied, an initial photocurrent density of 1.0 mA cm^{-2} is found, which decays quickly to 0.08 mA cm^{-2} after illumination for 10 s (black line in Figure 2). While a 0.2 V external bias is applied, a higher initial photocurrent density of 1.5 mA cm^{-2} and a higher final photocurrent density of ~0.48 mA cm^{-2} are observed (red line in Figure 2). When a higher external bias, such as 0.50 V, is applied, the initial and final photocurrent densities are found to

dx.doi.org/10.1021/cs500518k | ACS Catal. 2014, 4, 2347−2350

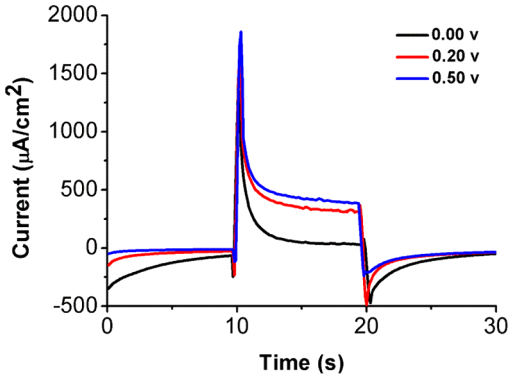

Figure 2. Photocurrent measurements of a three-electrode PEC upon application of different biases, with TiO_2(**1**+**2**) as the working electrode, in a 0.1 M Na_2SO_4 solution under illumination with a 300 W xenon lamp through a 400 nm long-pass filter (300 mW/cm^2).

be 1.6 and 0.5 mA cm^{-2}, respectively (blue line in Figure 2). When 0.2 and 0.5 V external biases are applied, no significant difference in the photocurrent densities of the PEC devices is observed.

In addition, CV measurements of the WEs under illumination were also conducted as shown in Figure S2a of the Supporting Information. The photocurrent density of WE TiO_2(**1**+**2**) reaches its maximum at an ∼0.2 V bias (vs the NHE), and no further increase in photocurrent density with higher potentials (Figure S2a of the Supporting Information, black line). The result is in a good agreement with the measurements of photocurrent densities performed at different biases shown in Figure 2. The photocurrent densities of WEs TiO_2(**1**) (Figure S2a of the Supporting Information, blue line) and TiO_2(**2**) (Figure S2a of the Supporting Information, red line) are found to be extremely low. Nearly no further increase in the photocurrent densities can be observed with increasing potentials. Therefore, an external bias of 0.2 V (vs the NHE) is adopted in the following studies.

The photocurrent measurements of PECs in a 0.1 M Na_2SO_4 solution were performed under a 0.2 V external bias versus the NHE, as shown in Figure 3. The PEC with WE TiO_2(**1**+**2**) as a photoanode displays high initial and final photocurrent densities after illumination for 10 s (blue line). Under the same conditions, photocurrent densities of WEs TiO_2(**1**) (red line), TiO_2(**2**) (black line), and TiO_2(**1**+**2a**) (green line) were found to be very low. The results show the PS, catalyst, and Zr^{4+} ion are all necessary for a photoanode to keep the PEC working more efficiently.

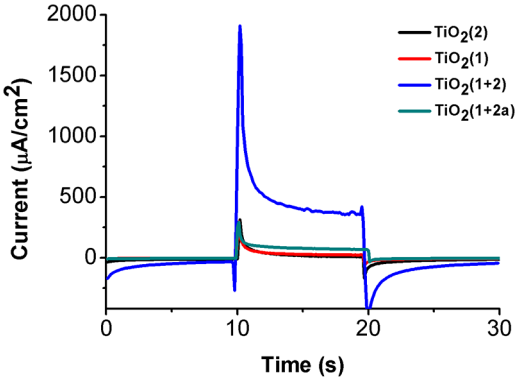

Figure 3. Photocurrent measurements of PECs (0.8 cm^2) in a 0.1 M Na_2SO_4 solution with an external bias (0.2 V vs the NHE) upon light illumination with a 300 W xenon lamp white light source coupled to a 400 nm long-pass filter (300 mW/cm^2), with working electrodes TiO_2(**1**+**2**) (blue), TiO_2(**1**) (red), TiO_2(**2**) (black), and TiO_2(**1**+**2a**) (green).

The light control measurement shows that the PEC devices maintain a high photocurrent density for several illumination cycles as shown in Figure 4. Long-term illumination measurements on water splitting were conducted for the PEC devices based on WE TiO_2(**1**+**2**) (Figure S4 of the Supporting Information). Hydrogen and oxygen gases were observed as small bubbles on respective electrode surfaces during the measurements and confirmed qualitatively by gas chromatography as shown in Figure S5 of the Supporting Information. It is difficult to measure the amounts of the generated gases accurately because the gases are generated in small amounts, some bubbles being stuck to electrodes and some dissolved in the solution. Nevertheless, from a rough calculation, the ratio of hydrogen to oxygen produced was found to be quite close to 2:1.

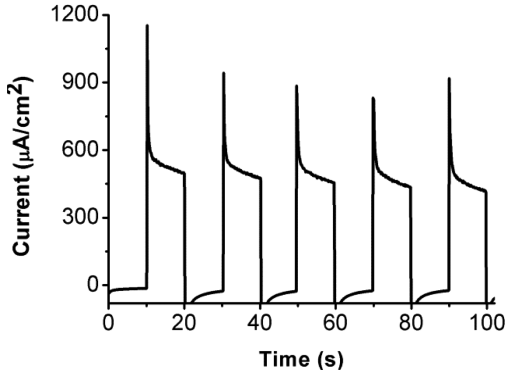

Figure 4. Light control photocurrent density measurement of the PEC with TiO_2(**1**+**2**) as the working electrode in a 0.1 M Na_2SO_4 solution (pH 6.4) with a 0.2 V bias vs the NHE with a 300 W xenon lamp through a 400 nm long-pass filter (300 mW/cm^2).

The incident photon to current conversion efficiency (IPCE) as an important parameter for the PEC's performance was also measured by using WE TiO_2(**1**+**2**) as a photoanode. A maximal IPCE value of 4.1% is obtained at ∼450 nm (Figure 5, black line). Such low IPCE values further reflect the low photocurrent density as described previously in the photocurrent measurements. The IPCE values are strongly correlated to the

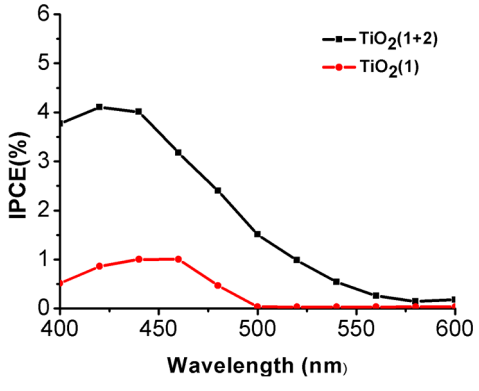

Figure 5. IPCE spectra of the PECs in 0.1 M Na_2SO_4 solutions (pH 6.4) with a 0.2 V external bias vs the NHE.

dx.doi.org/10.1021/cs500518k | ACS Catal. 2014, 4, 2347−2350

conversion efficiency of the absorbed photons to electrons, also known as the absorbed photon to current efficiency (APCE). APCE values strongly depend on the electron injection yield, dye regeneration yield, and charge collection efficiency. One could deduce that either insufficient electron injections, lower dye regeneration yields, or faster charge recombination between the electrons in the conduction band of TiO_2 and the supramolecular assembly should account for such lower observed IPCE values, and thus lower photocurrents. The reasons to explain the lower photocurrent density and IPCE values observed for the PEC devices need to be systematically studied in the future.

In summary, a working electrode has been successfully assembled by using a facile supramolecular self-assembly method. Through a Zr^{4+} ion, a molecular catalyst **2** was readily connected to a molecular PS **1**, the anchoring group of which was attached to a nanostructured TiO_2 photoanode. By using this photoanode in a three-electrode system, the PEC displayed a maximal IPCE value of 4.1% at ∼450 nm, and a photocurrent density of ∼0.48 mA cm^{-2} during the long-term light control measurements. Although mediocre photocurrent density and IPCE values were observed for the PEC devices, the work presented here still interestingly offers a new platform for constructing "monolayer" molecular devices using a supramolecular self-assembly method. Further studies of electron transfer processes in the working electrode are underway. The exploration of a superior linkage between the catalyst and the PS is also underway to further improve the performance of this type of molecular device for light-driven water splitting.

■ ASSOCIATED CONTENT

Supporting Information

Full experimental details, control experiments, experimental methods, and Figures S1−S3. This material is available free of charge via the Internet at http://pubs.acs.org.

■ AUTHOR INFORMATION

Corresponding Authors

*E-mail: dr.gaoyan@dlut.edu.cn.
*E-mail: lichengs@kth.se.

Notes

The authors declare no competing financial interest.

■ ACKNOWLEDGMENTS

This work was supported by the National Basic Research Program of China (973 program) (2014CB239402), the National Natural Science Foundation of China (20923006, 21003017, 21120102036, 21106015, and 91233201), the Fundamental Research Funds for the Central Universities, the Swedish Energy Agency, and the K&A Wallenberg Foundation.

■ REFERENCES

(1) Grätzel, M. *Nature* **2001**, *414*, 338−344.
(2) Youngblood, W. J.; Lee, S.-H. A.; Kobayashi, Y.; Hernandez-Pagan, E. A.; Hoertz, P. G.; Moore, T. A.; Moore, A. L.; Gust, D.; Mallouk, T. E. *J. Am. Chem. Soc.* **2009**, *131*, 926−927.
(3) Youngblood, W. J.; Lee, S.-H. A.; Maeda, K.; Mallouk, T. E. *Acc. Chem. Res.* **2009**, *42*, 1966−1973.
(4) Nann, T.; Ibrahim, S. K.; Woi, P. M.; Xu, S.; Ziegler, J.; Pickett, C. J. *Angew. Chem., Int. Ed.* **2010**, *49*, 1574−1577.
(5) Townsend, T. K.; Sabio, E. M.; Browning, N. D.; Osterloh, F. E. *Energy Environ. Sci.* **2011**, *4*, 4270−4275.
(6) Kronawitter, C. X.; Vayssieres, L.; Shen, S.; Guo, L.; Wheeler, D. A.; Zhang, J. Z.; Antoun, B. R.; Mao, S. S. *Energy Environ. Sci.* **2011**, *4*, 3889−3899.
(7) Barroso, M.; Cowan, A. J.; Pendlebury, S. R.; Grätzel, M.; Klug, D. R.; Durrant, J. R. *J. Am. Chem. Soc.* **2011**, *133*, 14868−14871.
(8) Maeda, K.; Higashi, M.; Siritanaratkul, B.; Abe, R.; Domen, K. *J. Am. Chem. Soc.* **2011**, *133*, 12334−12337.
(9) Higashi, M.; Domen, K.; Abe, R. *Energy Environ. Sci.* **2011**, *4*, 4138−4147.
(10) Higashi, M.; Domen, K.; Abe, R. *J. Am. Chem. Soc.* **2012**, *134*, 6968−6971.
(11) Reece, S. Y.; Hamel, J. A.; Sung, K.; Jarvi, T. d.; Esswein, A. J.; Pijpers, J. J. H.; Nocera, D. G. *Science* **2011**, *334*, 645−648.
(12) Moore, G. F.; Blakemore, J. D.; Milot, R. L.; Hull, J. F.; Song, H.; Cai, L.; Schmuttenmaer, C. A.; Crabtree, R. H.; Brudvig, G. W. *Energy Environ. Sci.* **2011**, *4*, 2389−2392.
(13) Li, L.; Duan, L.; Xu, Y.; Gorlov, M.; Hagfeldt, A.; Sun, L. *Chem. Commun.* **2010**, *46*, 7307−7309.
(14) Zhao, Y.; Swierk, J. R.; Megiatto, J. D., Jr.; Sherman, B.; Youngblood, W. J.; Qin, D.; Lentz, D. M.; Moore, A. L.; Moore, T. A.; Gust, D.; Mallouk, T. E. *Proc. Natl. Acad. Sci. U.S.A.* **2012**, *109*, 15612−15616.
(15) Glasson, C. R. K.; Song, W.; Ashford, D. L.; Vannucci, A.; Chen, Z.; Concepcion, J. J.; Holland, P. L.; Meyer, T. J. *Inorg. Chem.* **2012**, *51*, 8637−8639.
(16) Ashford, D. L.; Song, W.; Concepcion, J. J.; Glasson, C. R. K.; Brennaman, M. K.; Norris, M. R.; Fang, Z.; Templeton, J. L.; Meyer, T. J. *J. Am. Chem. Soc.* **2012**, *134*, 19189−19198.
(17) Hanson, K.; Torelli, D. A.; Vannucci, A. K.; Brennaman, M. K.; Luo, H.; Alibabaei, L.; Song, W.; Ashford, D. L.; Norri, M. R.; Glasson, C. R. K.; Concepcion, J. J.; Meyer, T. J. *Angew. Chem., Int. Ed.* **2012**, *51*, 12782−12785.
(18) Xiang, X.; Fielden, J.; Rodríguez-Córdoba, W.; Huang, Zh.; Zhang, N.; Luo, Zh.; Musaev, D.; Lian, T.; Hill, C. *J. Phys. Chem. C* **2013**, *117*, 916−918.
(19) Gao, Y.; Ding, X.; Liu, J.; Wang, L.; Lu, Z.; Li, L.; Sun, L. *J. Am. Chem. Soc.* **2013**, *135*, 4219−4222.
(20) Duan, L.; Bozoglian, F.; Mandal, S.; Stewart, B.; Privalov, T.; Llobet, A.; Sun, L. *Nat. Chem.* **2012**, *4*, 418−423.
(21) Duan, L.; Fischer, A.; Xu, Y.; Sun, L. *J. Am. Chem. Soc.* **2009**, *131*, 10397−10399.
(22) Li, F.; Jiang, Y.; Zhang, B.; Huang, F.; Gao, Y.; Sun, L. *Angew. Chem., Int. Ed.* **2012**, *51*, 2417−2420.
(23) Duan, L.; Xu, Y.; Gorlov, M.; Tong, L.; Andersson, S.; Sun, L. *Chem.—Eur. J.* **2010**, *16*, 4659−4668.
(24) Chen, Z.; Concepcion, J. J.; Jurss, J. W.; Meyer, T. J. *J. Am. Chem. Soc.* **2009**, *131*, 15580−15581.
(25) Nakayama-Ratchford, N.; Bangsaruntip, S.; Sun, X.; Welsher, K.; Dai, H. *J. Am. Chem. Soc.* **2007**, *129*, 2448−2449.
(26) Ishida, T.; Terada, K.-i.; Hasegawa, K.; Kuwahata, H.; Kusama, K.; Sato, R.; Nakano, M.; Naitoh, Y.; Haga, M.-a. *Appl. Surf. Sci.* **2009**, *255*, 8824−8826.